

Effect of Nano B₄C on the Tribological Behaviour of Magnesium Alloy Prepared Through Powder Metallurgy

Sankar CHINTHAMANI¹, Gangatharan KANNAN¹, Glan Devadhas GEORGE²,
Christopher Ezhil Singh SREEDHARAN^{3*}, Krishna Sharma RAJAGOPAL⁴

¹ Department of Mechanical Engineering, PSN College of Engineering and Technology, Tirunelveli-627152, Tamilnadu, India

² Department of Mechanical Engineering, Vimal Jyothi Engineering College, Chemperi, Kannur -670632, Kerala, India

³ Department of Applied Electronics and Instrumentation Engineering, Vimal Jyothi Engineering College, Chemperi, Kannur -670632, Kerala, India

⁴ Department of Physics, St.Hindu College, Nagercoil-629002, Kanyakumari, India

crossref <http://dx.doi.org/10.5755/j01.ms.26.4.21556>

Received 01 September 2019; accepted 26 November 2019

In this present study, the particle size of as received magnesium alloy (AZ91) and B₄C powders was reduced through high energy ball mills. The combination of AZ91 (both 10 μm and 60 μm) reinforced with nano B₄C particles were fabricated by powder metallurgy technique. The incorporation of nano B₄C particles to the Mg matrix was done at various weight % such as 5, 10, 15 and 20. The AZ91 composites were fabricated in a suitable die set assembly and the green compacts were sintered in an electric muffle furnace at 500 °C with argon atmosphere for a dwell time of 1 h. The density of the composites was estimated using Archimedes principle. Micro hardness test was carried out for the prepared specimens and dry sliding wear test was conducted by using pin-on-disc apparatus at room temperature with varying loads and sliding velocities by keeping a constant Sliding Distance (SD). Among the various specimens, the composite with 10 μm size attained a higher Vickers hardness value as well as better wear resistant property. Worn surface analysis of the prepared composites was studied using Scanning Electron Microscope (SEM).

Keywords: AZ91, B₄C, coefficient of friction, sliding wear, hardness.

1. INTRODUCTION

There is much attention in scientific research because of the increase in demand on lightweight materials for aerospace and automotive applications. Metal matrix composites are used as effective reinforcements to enhance the mechanical properties and also reduction in fuel consumption [1, 2]. Many researchers found that magnesium alloys process good strengthening affects and are used in aerospace applications due to its low density. Magnesium composites result in better wear resistance and lower Coefficient of Friction (CoF) [3]. Recent works focused on AZ91 magnesium alloy, which has good mechanical properties, Specific Wear Rate (SWR) and hardness [4]. Powder metallurgy method utilizes reduced manufacturing temperature and gains uniform reinforcement distribution. So, metal matrix composites (MMC's) were prepared by this method which favours nucleation at the reinforcement-matrix interface [5].

Magnesium alone has reduced lifetime, poor corrosion resistance and wear property but it's lightweight and low density makes the material demand and applicable for automobile and aerospace.

It can be reinforced with matrix composites like aluminium, boron carbide, silicon carbide, titanium carbide, etc. [6]. Also, the mechanical properties of pure

magnesium and its alloys were improved by high strength and high modulus materials like titanium, zinc, copper and nickel etc., Researchers found compressive responses when Mg is incorporated with ZrO₂ and Cu led to enhanced hardness, compressive and tensile strength [7, 8]. Also, silicon carbide reinforced Mg composites processed by powder metallurgy technique enhances the compressive behaviour with reduced grain size and uniform reinforcement distribution [9]. The microstructures of Mg sample changes with average grain size and weight percentage of the reinforcements added [10]. The reinforcement of nanoparticles to the magnesium composites exhibits superior mechanical properties such as hardness, corrosion resistance and tribological behaviour [11].

In this research, AZ91 magnesium alloy is reinforced with Boron carbide in different weight percent to reduce the wear rate and CoF. B₄C is a one of the carbide particles, which is used to increase the strength and tribological properties [12]. Specially, the interfacial microstructure was focused on many studies such as aluminium composites reinforced with boron carbide, which results in high strength, low density, high hardness and Young's modulus [13]. Ball milling was carried out for homogeneous mixing of nano B₄C particles with AZ91 alloy for 1h before taken to compaction. The AZ91 alloy reinforced with B₄C particles were prepared through powder metallurgy method [14]. The compacted specimen

* Corresponding author. Tel.: +91-8300352566.

E-mail address: edbertefren0420@gmail.com (C.E.S. Sreedharan)

with various proportions of nano B₄C particles is then consolidated for sintered and after sintering Mg based composites possesses better hardness and strength, therefore, the incorporated reinforcement plays an important role in physical properties [15].

In this present study, various concentrations of nano B₄C particles reinforced AZ91 alloy with varying particle sizes have been alloyed by ball milling to improve the dispersion of secondary particle followed by powder metallurgy techniques (Compaction and sintering). The microstructure evolution of sintered AZ91-B₄C nanocomposites has been studied in detail using scanning electron microscopy (SEM) analysis. Further, the SWR and CoF of the prepared nanocomposites have been investigated. These nanocomposites could be a better candidate in wider application such as automobiles and electrical components.

2. MATERIALS AND EXPERIMENTAL TECHNIQUES

2.1. Mechanical milling of powders

As AZ91 and B₄C were the nominees for the size reduction process, tedious ball milling process was carried out. The high energy ball mill (Fritsch, Pulverisette 6, Germany) having WC jar and having the same material balls (diameter 10 mm) were used. Mg alloy AZ91 contains a major composition of Magnesium. The weight ratio of ball to powder was taken as 20:1. In order to avoid the oxidation during milling, 2 wt.% of stearic acid with methanol was added to the powder samples and also the entire milling process was carried out in an inert gas (argon) atmosphere condition. Stearic acid is an organic compound which easily undergoes vaporization upon absorbing heat energy in room temperature itself [10]. As milling generates heat energy, this favors the lowering in level of the process control agent (PCA) inside the milling container. The Mg alloy AZ91 powder with an average particle size of 60 μm was milled for 18 h. On behalf of this, an interruption in milling is done at every 0.25 h to ensure the optimum heat level. B₄C was further milled to nano level for 50 h by following the mentioned above protocol. Organic contaminations left out after this wet milling process while the samples are drying in the hot air oven for 2 h at 120 °C. Now nano sized precursors are quite ready for further processing.

2.2. Materials

The commercially available magnesium alloy AZ91 was used in this work and has an average particle size of 60 μm was received from Sigma Aldrich, Germany. Boron Carbide powder was used as reinforcement and it was purchased from Sigma Aldrich, Germany with an average particle size of 10 μm. Fig. 1 a shows the SEM images of as received Mg alloy AZ91 which displays the morphology of curved ribbon like flake structure.

The chemical composition of AZ91 alloy is 90 %Mg, 9 % Al and 1 % Zn respectively. Fig. 1 b shows the AZ91 alloy after milling about 18 h. During milling the sharp flakes has broken due to the strain hardening and it turned into broken flakes.

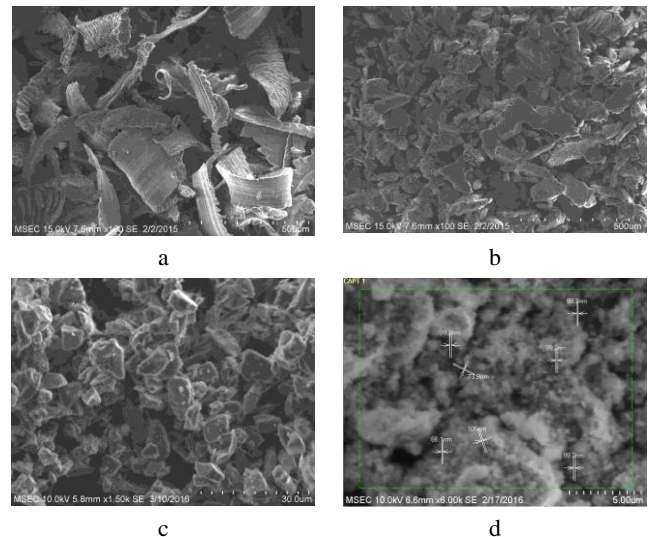


Fig. 1. SEM micrographs showing: a—as received powder of AZ91 alloy; b—after milling AZ91 alloy; c—as received powder of B₄C; d—after milling B₄C

Fig. 1 c shows the morphology of as received boron carbide particles which has small flake-like structure and the density is 2520 kg/m³. Fig. 1 d shows the milled B₄C particles after 50 h milling. It is perceived from the images that, in the method of ball milling the powders strike with the grinding balls forming high pulverization energy accountable for introducing lattice flaws that cause the powder particles to converge and deform plastically. While continuing the process, the powder particles fracture and the reinforce particles are cold welded. Further the expansion of the forming particles with reinforcement as an intermediary phase appearing inside or at the surface of these particles as shown in Fig. 1 d. It is also found that the particles are splintered again into submicron matrix particles with the ultra-fine dispersal of the reinforcement phase [10].

2.3. Microstructural characterization

X-ray diffraction (XRD) patterns of AZ91 nanocomposite were recorded by Philips PW3040/60 X-ray generator diffractometer in the diffracting angles between 20°–80° with a step size of 3°/min. The scanning electron microscopy (SEM, HITTACHI SU1510) was used for the microstructural analysis of powder and wear measured samples. Microstructural characterization studies were directed on standard metallographically polished with an aid of SiC abrasive paper and afterwards a finer diamond paste to yield a mirror-like surface.

2.4. Wear test

The dry sliding wear test was conducted with the help of pin-on-disc tribometer (Ducom, Bangalore) in accordance to the ASTM: G99-05 under various applied load of 5 to 25 N with increment of 5 N at constant velocity of 2.61 m/s with constant sliding distance of 1500 m. Prior to each testing, the specimen and counter face disc were wiped using acetone to eliminate the traces. The frictional force was noted from the digital micrometre and coefficient of friction was also calculated. Wear worn testing on the surface morphology of magnesium alloy

AZ91 was observed from the SEM. To determine the CoF in order to varying the load, sliding velocity and constant sliding distance. The samples contact surface was flat and in contact with the rotating disc. The test was performed by applying load on the pin against the EN31 steel disc. Then the load was applied which acts as a counter weight and helps in balancing the pin. The track radius or track diameter was kept constant for each trial conducted by varying the machine parameters such as load, sliding velocities and sliding distance. Once the sample surface was setup to contact with the disc for the selected reinforcement, load, sliding distance and sliding velocity the SWR and CoF were measured [4, 5].

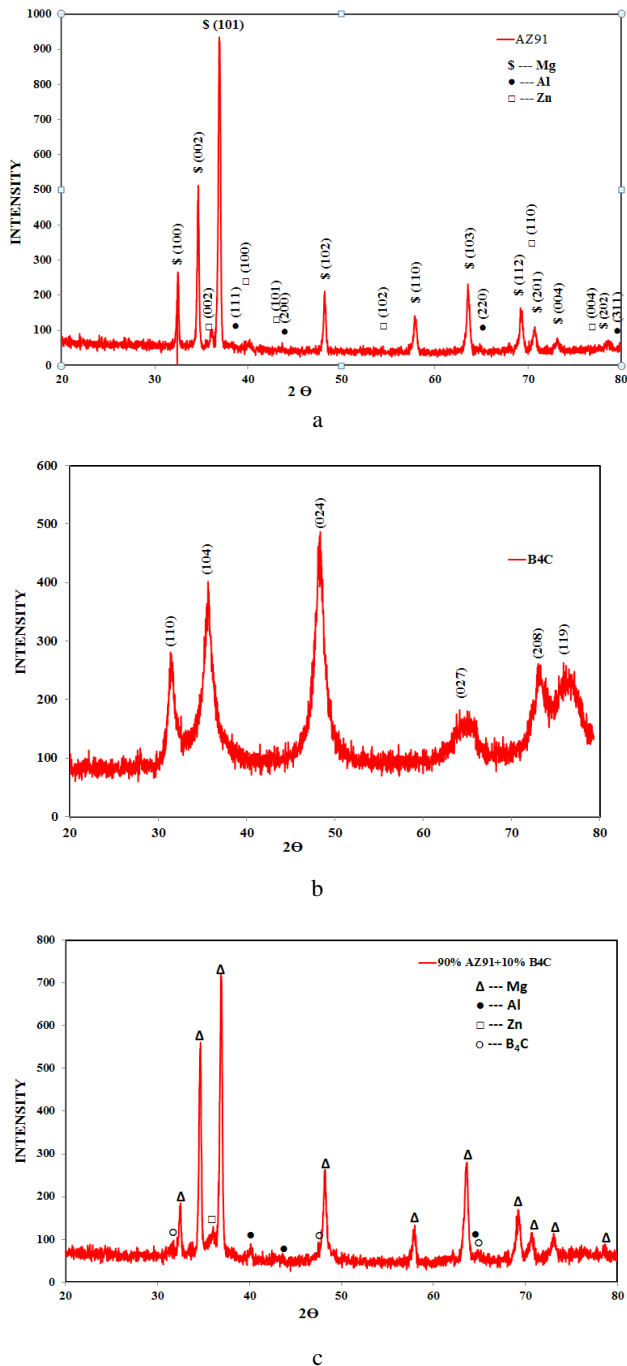


Fig. 2. XRD analysis: a–AZ 91 alloy; b–milled nano B₄C; c–AZ 91 alloy-10B₄C composite.

3. RESULTS AND DISCUSSION

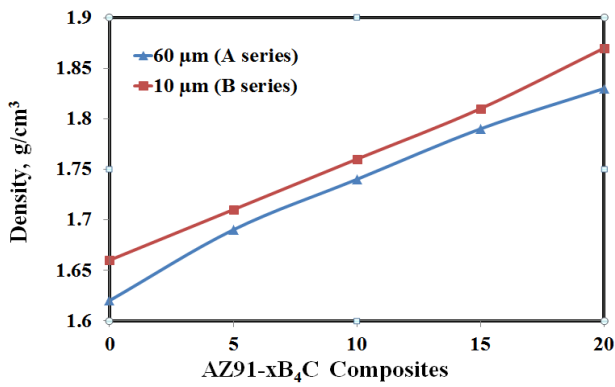
3.1. XRD characterization

Fig. 2 shows the x ray diffraction results of AZ91 alloy, B₄C and AZ91-10B₄C composite. The X-rays used to diffract the samples were generated by a Cu-K α radiation source ($\lambda = 1.54060 \text{ \AA}$) with a step size of 0.02° . The samples were analyzed over a range of angles from 20 to 80° . AZ91 is an alloy composed of 9 % aluminium, 1 % zinc and remaining 90 % magnesium. Fig. 2 a shows the characteristic sharp peaks located at 36.9 , 38.1 and 43.2 corresponding to Mg, Al, Zn respectively (JCPDS No: 894894, 851327 & 870713) and proves that the formation of AZ91 alloy. Crystal plane index was found for magnesium, aluminium and zinc such as (101), (111) and (100). This is evident from the same JCPDS file number 894894, 851327 & 870713 respectively. The intensity of diffraction peaks corresponds to Al and Zn is very low compared to Mg due to their minimum weight percentage proportion. There were no impurity peaks rather than the characteristic of B₄C peak [7]. Fig. 2 b and also shows that the characteristic sharp peaks located at 31.39 , 35.67 , 48.27 , 72.94 , and 75.9 corresponds to B₄C respectively (JCPDS No: 750424). Crystal plane index was found for boron carbide B₄C such as (110), (104), (024), (027), (208) and (119).

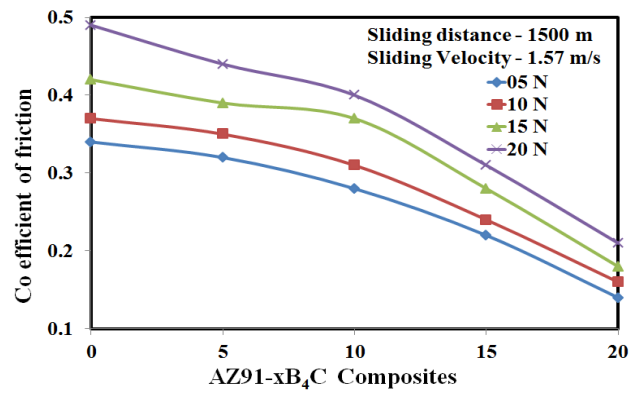
Fig. 2 c contains the both characteristic diffraction peaks for AZ91 and B₄C indicates the formation of AZ91-10B₄C composite. Due to the presence of individual peaks in XRD analysis, the composite formation is confirmed without any unnecessary phase formations [15]. The XRD pattern in Fig. 2 c shows a sharp diffraction peak at angular position 36.7 along the prominent reflection (101) corresponds to Mg element. In addition to some other lower intense diffraction peaks corresponds to Mg element also observed in 2θ value 32.2 , 34.5 , 36.7 , 48.0 , 57.59 , 63.2 , 68.8 , 70.2 , 72.7 and 77.4 . Besides this major element, three more elements such as Al, Zn and B₄C also observed in the diffraction pattern of AZ91-10B₄C composite. The reflections along 2θ value about 31.81 , 40.13 and 64.53 are corresponds to B₄C, 38.7 , 44.5 and 65.3 are corresponds to Al and 35.95 and 35.65

3.2. Density and hardness

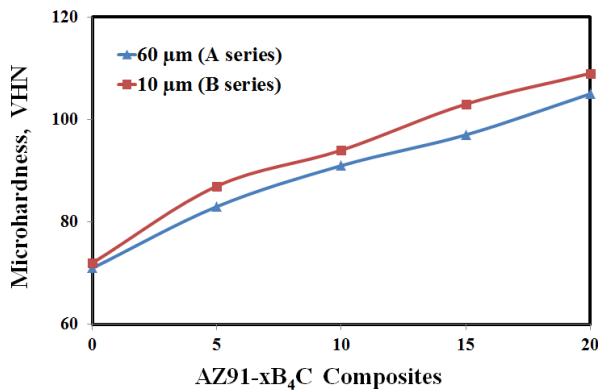
Fig. 3 a shows that the density of the sintered nanocomposites pellets was measured using the Archimedes principle as per the ASTM standard: B962-08 for the particle sizes $60 \mu\text{m}$ and $10 \mu\text{m}$. The porosity in all the nanocomposites was lesser than that in Mg AZ91 alloy. A small increase in the density of the nanocomposites was detected with increasing the addition of nano B₄C or the decreases in porosity in the Mg matrix. Fig. 3 b it can be noticed that micro-hardness of AZ91-B₄C nanocomposites were measured by applying load of 0.025 kg for indentation for 15 s dwell time [9]. Fig. 3 it illustrates that compare to the $60 \mu\text{m}$ sizes $10 \mu\text{m}$ size composites are having better density and hardness irrespective of the size of the particles. It was observed that the density and hardness of Mg AZ91 alloy linearly increase when the reinforcement particulates increases.



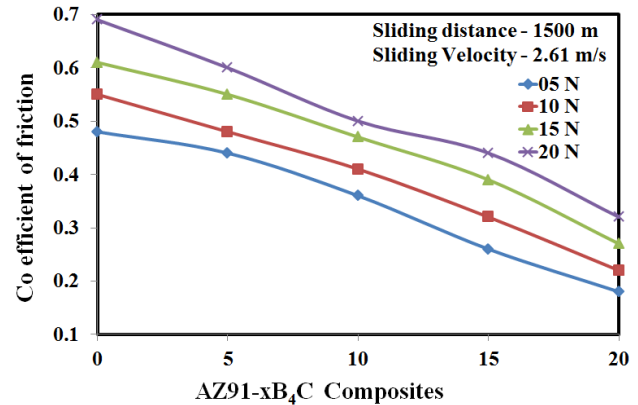
a



a



b



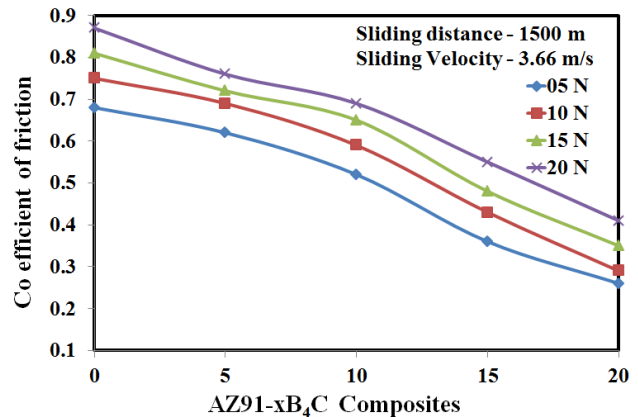
b

Fig. 3. The effect of AZ91-B₄C nanocomposites particulates: a – density; b – micro-hardness

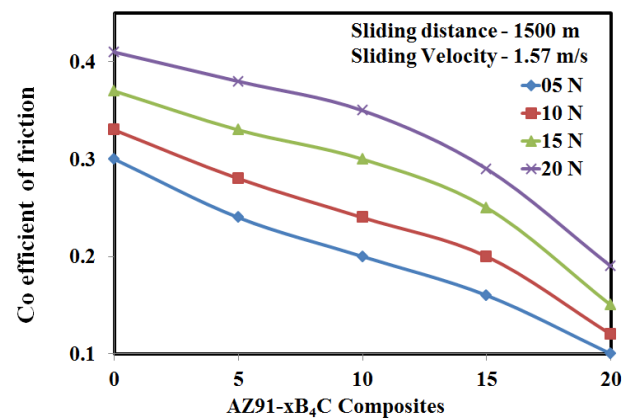
In addition to that secondary particles in the matrix increase the surface area of the reinforcement and the matrix grain sizes are abridged. The presence of such hard surface area of particles leads to increase the hardness of the composites due to the resistance of plastic deformation of the particles. The presence of hard ceramic phase in the soft matrix reduces the ductility of composites due to reduction of ductile metal content which expressively increases the hardness value [13].

3.3. Coefficient of friction as a function of reinforcement

In this research, AZ91 alloy is a matrix and B₄C as the reinforcement added to enhance the tribological property of the composites. Several works are having carried out to reduce wear by incorporating double reinforcement. In this work, single reinforcement is added to reduce SWR. By varying the weight fraction of reinforcement, sliding velocity and applied load the CoF were measured. From Fig. 4, it is evident that drop in CoF was monitored by various parameters such as load applied (20 N), sliding velocities and sliding distance of 1500 m. Among all the parameters, load applied is the dominant factor on the CoF. Under different loading condition and sliding velocity with constant sliding distance, CoF is more for AZ91 alloy and lesser while B₄C reinforcement is added. The reason is that Mg alloy is a smooth material which easily undergoes wear [7–9]. So the addition of hard reinforcement material (B₄C) results in dropping of CoF.



c



d

continued on next page

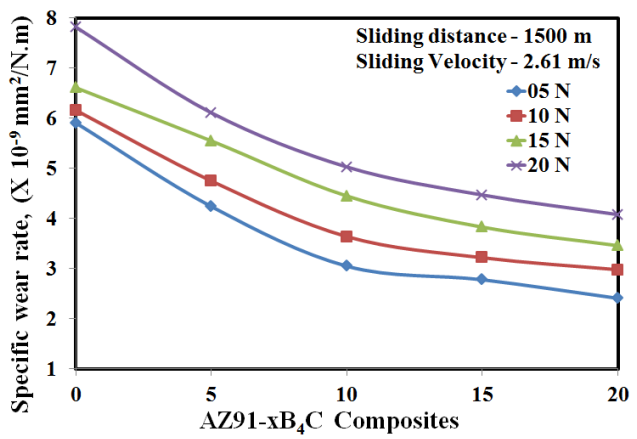
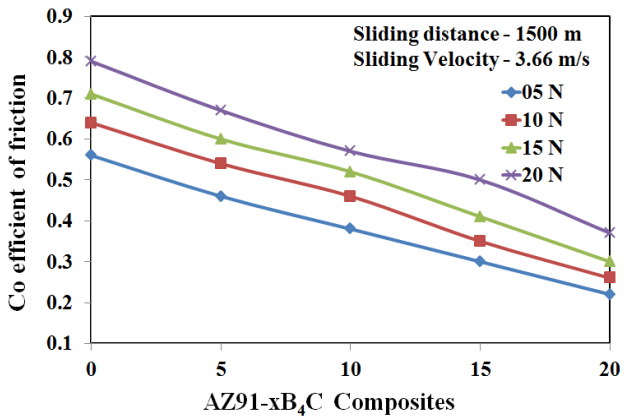
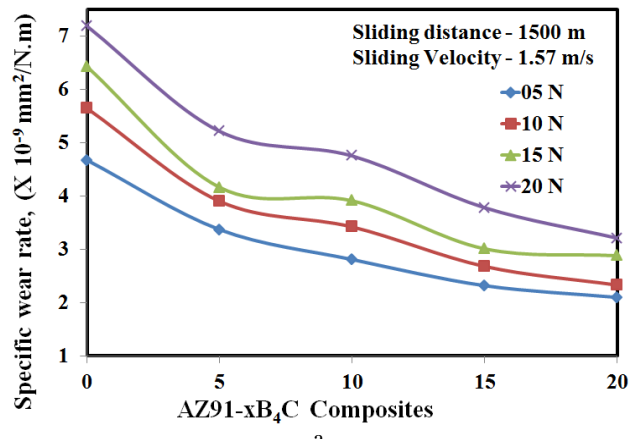
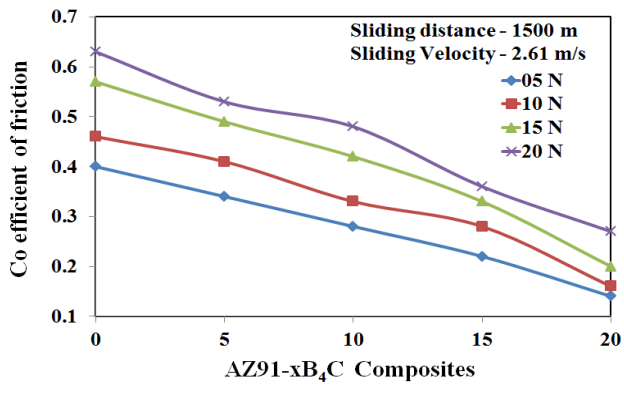
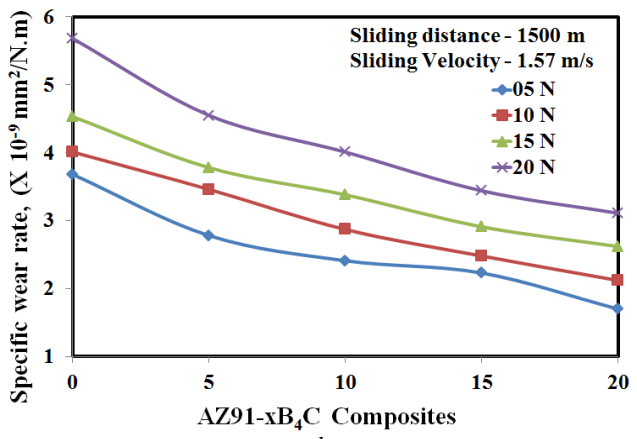
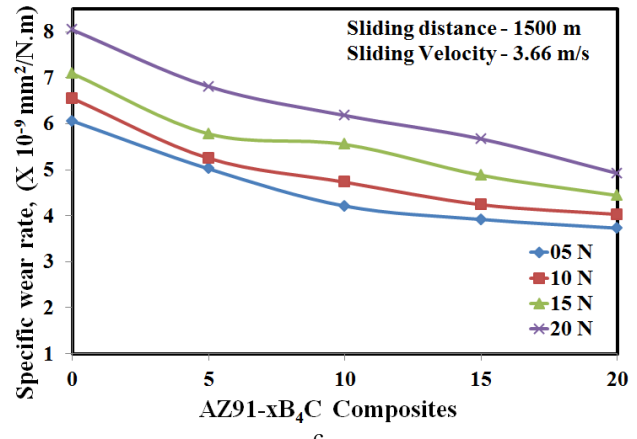


Fig. 4. Co-efficient of friction of AZ91 composite with varying B₄C content, particle size and speed: a – 60 μm 300 rpm; b – 60 μm 500 rpm; c – 60 μm 700 rpm; d – 10 μm 300 rpm; e – 10 μm 500 rpm; f – 10 μm 700 rpm

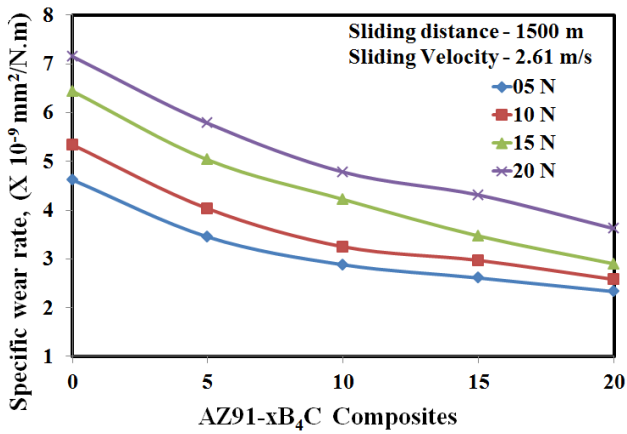
From the graph, it is noticed that the gradual and steady increase of curve confirms that the CoF increases with maximum sliding velocity and load applied on the material. It is proven that at the initial stage, the applied load is less. Hence the CoF is also less; because of the fact that load is the one of the dominant factor to increase the CoF. From the graph it is also proven that when compared to 60 μm composites, 10 μm composite specimens has less CoF because of high surface to volume ratio of the AZ91 alloy. Further the specimen with AZ91-20B₄C, 10 μm and 3.66 m/s has less CoF than the other type of composites is due to the hard ceramic secondary particle.

3.4. Specific wear rate as a function of reinforcement concentration

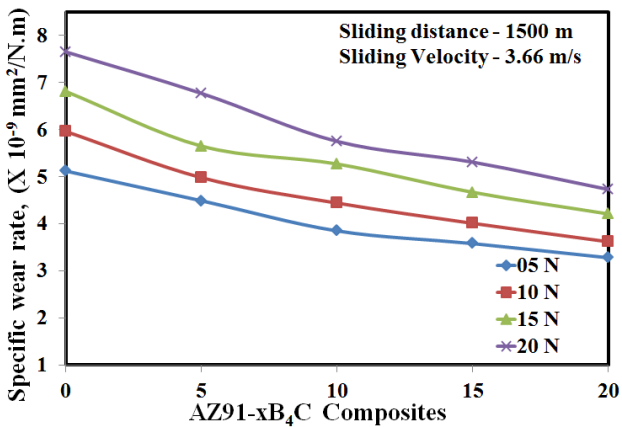
The experiment was carried out in a pin-on-disc test setup. The test was conducted on a track for particular time duration with applied load 5–20 N and constant sliding distances with constant track radius 100 mm and various sliding velocities. The MMCs of AZ91 alloy is incorporated with B₄C reinforcement to enhance the mechanical strength, hardness and reduce the friction and wear. Mg is a light metallic alloy and so it is not very much hard and lagging to withstand high temperature while conducting the wear experiment.



continued on next page



e



f

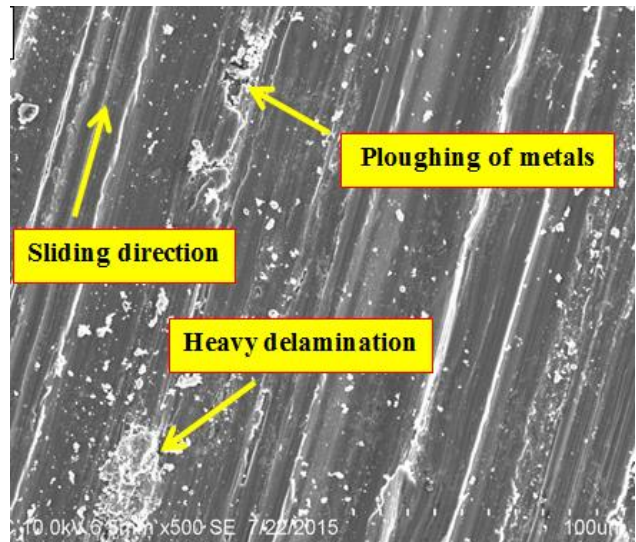
Fig. 5. Specific wear rate of AZ91 composite with varying B₄C content, particle size and speed: a – AZ9 160 μm 300 rpm; b – 60 μm 500 rpm; c – 60 μm 700 rpm; d – 10 μm 300 rpm; e – 10 μm 500 rpm; f – 10 μm 700 rpm

The SWR decreased with the incorporation of B₄C into the AZ91 alloy for 10 μm and 60 μm as shown in Fig. 5. The SWR exhibited an inverse trend, accompanying with an increase in amount of deformed wear debris. Excessive incorporation of B₄C in to AZ91 alloy resulted in great reduction of hardness and SWR because its phase is accompanied with large weight fraction of B₄C and applied load. Fig. 5 clearly indicates that variation of SWR under constant sliding distance with various sliding velocities. The SWR is more when it was individually observed for an alloy or matrix material. If it was reinforced with a hard material, the hardened layer between the pin and the counter surface minimizes the SWR of the composites. The graph indicates that the SWR is of about $4.73 \times 10^{-9} \text{ mm}^3/\text{N}\cdot\text{m}$ for 20 wt.% B₄C reinforcement is added to Mg alloy with 20 N load applied, 1500 m sliding distance and 3.66 m/s sliding velocity for 10 μm specimen. As the result of this change in parameter, the material exhibits less SWR and so applicable for automobile applications. So for the prepared composites AZ91-20B₄C, the SWR was less when compared to light metallic alloy. It was observed from this work that, as the % of reinforcement was enriched, the SWR was found to be decreased.

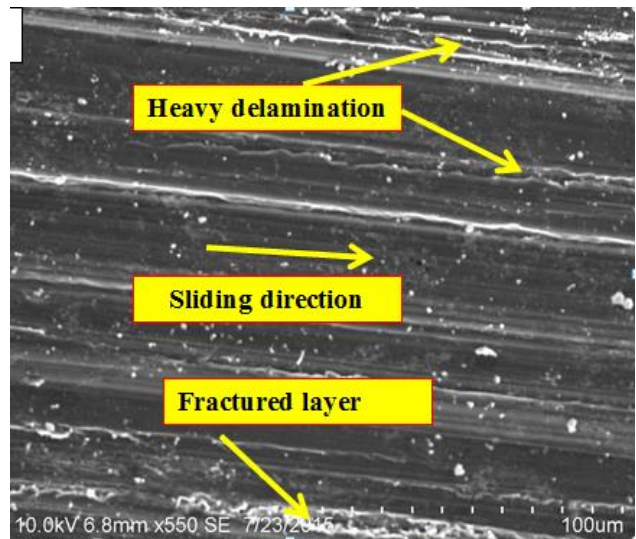
3.5. Worn surface analysis

Scanning Electron Microscopy observations were employed to examine the morphology of worn surface of the samples. From the SEM micrographs, one can observe the wear debris layer, smooth grooves, ploughing and roughening of surfaces. The worn surface of the composites is shown in Fig. 6. The SEM pattern indicates the formation of debris, grooves and oxide layer. The wear appeared for the composite was significantly differed from the unreinforced matrix. The specimen was tested under various loads and observed that reinforced composites were smoother and also the presence of some grooves at the worn surface [10–12].

There must be a considerable reduction in the plastic deformation due to increased hardness of the composites and increased plastic deformation with increasing the load. The formation of large wear at the pin surface results in fracture of reinforcements. Fig. 6 shows the worn surfaces of Mg AZ91 alloy and AZ91-20B₄C nanocomposites of both 60 and 10 μm respectively.

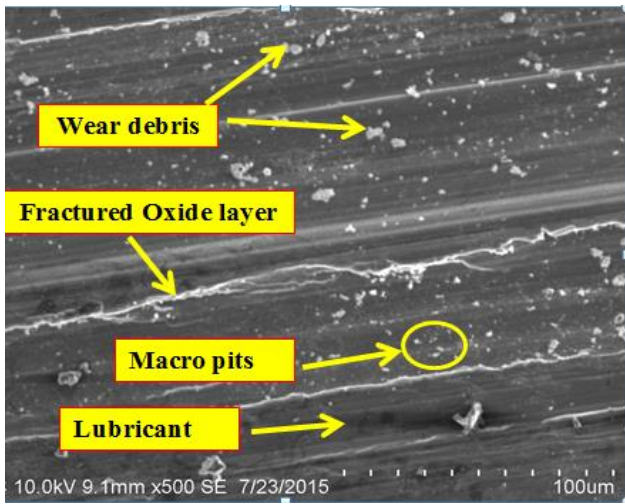


a

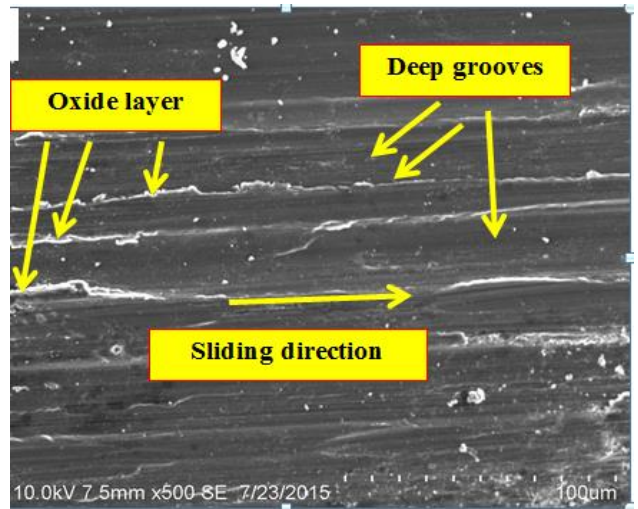


b

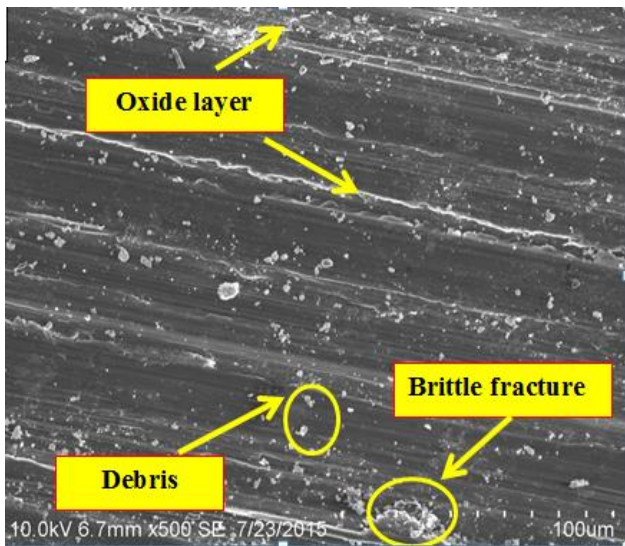
continued on next page



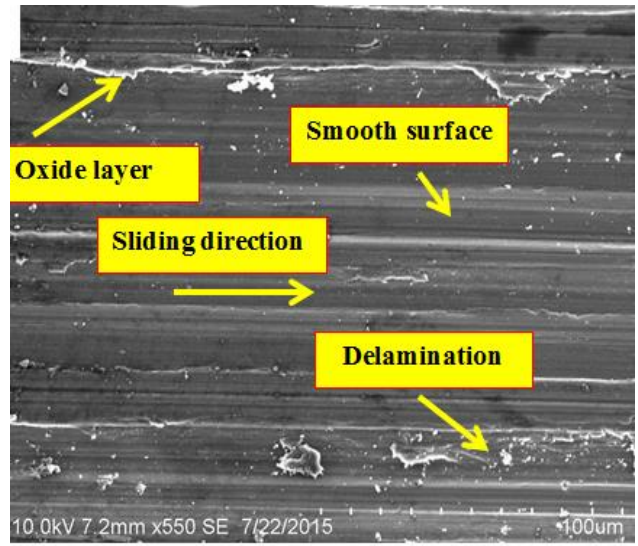
c



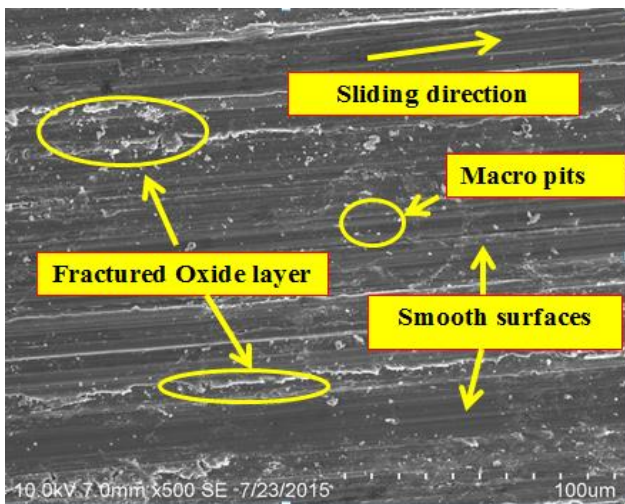
f



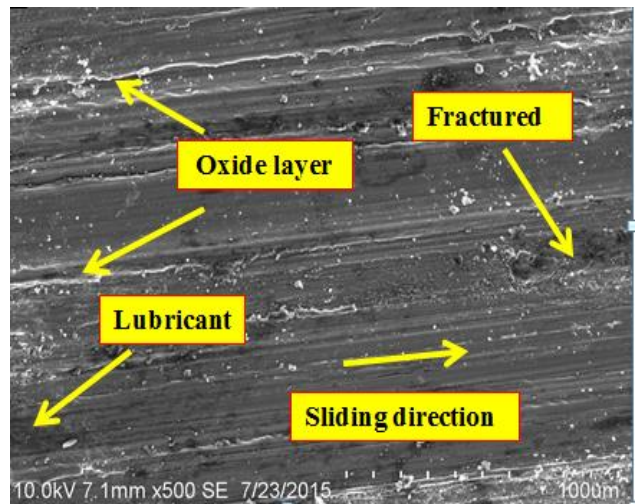
d



g

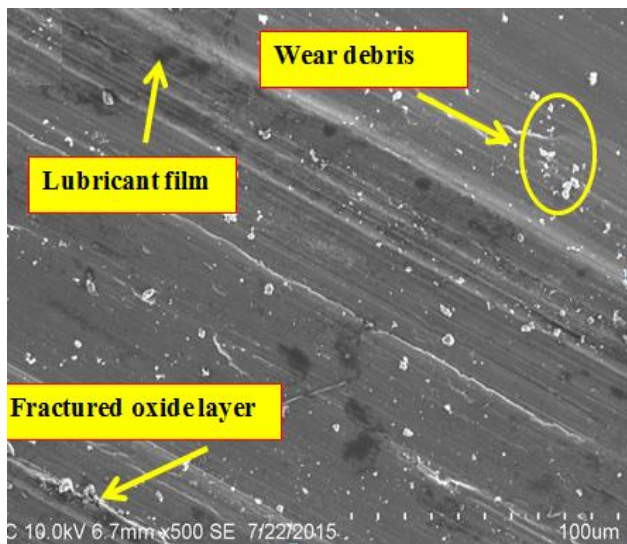


e

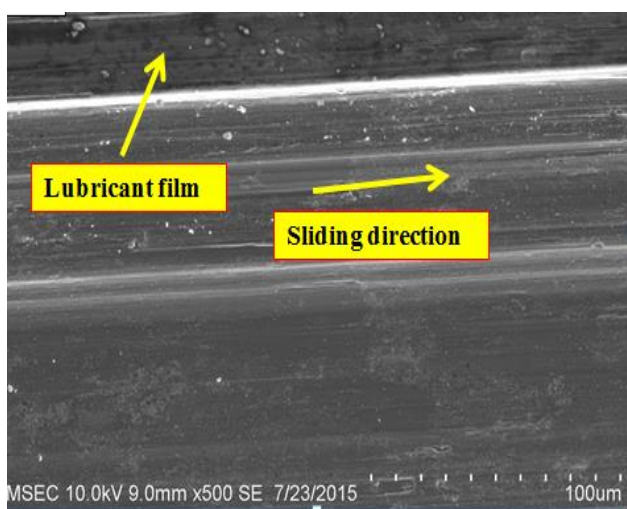


h

continued on next page



i



j

Fig. 6. SEM wear analysis of 60 μm composites: a–AZ91; b– AZ91 -5B₄C; c–AZ91-10B₄C; d–AZ91-15B₄C; e–AZ91-20B₄C; for 10 μm composites: f–AZ91; g–AZ91-5B₄C; h–AZ91-10B₄C; i–AZ91-15B₄C; j–AZ91-20B₄C

The worn surface of the composites tested at the sliding distance of 1500 m and at the applied load of 20 N inferred that the wear debris and delamination of the composites increases and ploughing depth is shallower for reduced % of reinforced materials whereas ploughing depth was reduced for higher % of reinforced material. Also, temperature plays a role in worn surface of the composite material i.e., at room temperature, grooves and ridges reduced considerably whereas the light material heated to a sintering temperature showed increased wear and higher depth of grooves was seen. From the above discussion it clearly indicates that 20 % of B₄C 10 μm has a prominent wear reduction property than the base alloy.

4. CONCLUSIONS

1. The improved properties were obtained (micro-hardness and density) for average particles size with 10 μm of AZ91 alloy when compared to the 60 μm

particle size of AZ91 alloy with reinforced nano B₄C in all the compositional percentages. These behaviors strongly suggest that particle size is one of the most influencing factors for enhancing the mechanical properties of AZ91 alloy composites.

2. From the observations, reinforcing B₄C in Mg matrix increases the wear resistance and strength of the base material. Nano B₄C reinforced composites exhibited a superior wear resistance than the unreinforced alloy.
3. The specific wear rate of the composites as well as the base alloy is increased irrespective of the applied load. Regular transitions from abrasion to adhesion and thus to delamination wear occurred with an increase in applied load.
4. The wear resistance of the composites depreciates as the presence of secondary phase promotes delamination wear. The transition to a high wear rate regime was prompted by surface damage and material transfer to the counter steel face.
5. The hard ceramic nano particles helped in delaying the transition to severe wear regime. However, to improve wear resistance, the nano B₄C reinforced AZ91 composites are possible candidate materials for wear resistance applications.

REFERENCES

1. Selvam, B., Marimuthu, P., Naraynassamy, R., Anandkrishnan, V. Dry Sliding Wear Behaviour of Zinc Oxide Reinforced Magnesium Matrix Nano Composites *Materials and Design* 58 2014: pp. 475–481. <https://doi.org/10.1016/j.matdes.2014.02.006>
2. Tun, K.S., Wong, W.L.E., Nguyen, Q.B., Gupta, M., Tensile and Compressive Responses of Ceramic and Metallic Nanoparticle Reinforced Mg Composites *Materials* 6 (5) 2013: pp. 1826–1839. <https://doi.org/10.3390/ma6051826>
3. Aung, N.N., Zhou, W., Goh, C.S., Nai, S.M.L., Wei, J. Effect of Carbon Nanotubes on Corrosion of Mg-CNT Composites *Corrosion Science* 52 (5) 2010: pp. 1551–1553. <https://doi.org/10.1016/j.corsci.2010.02.025>
4. Habibnejad-Korayem, M., Mahmudi, R., Ghasemi, H.M., Poole, W.J., Tribological Behavior of Pure Mg and AZ31 Magnesium Alloy Strengthened by Al₂O₃ Nanoparticles *Wear* 268 (3–4) 2010: pp. 405–412. <https://doi.org/10.1016/j.wear.2009.08.031>
5. Habibi, M.K., Paramsothy, M., Hamouda, A.M.S., Gupta, M. Enhanced Compressive Response of Hybrid Mg-CNT Nanocomposites *Journal of Materials Science* 46 (13) 2011: pp. 4588–4597. <https://doi.org/10.1007/s10853-011-5358-2>
6. Sankaranarayanan, S., Jayalakshmi, S., Gupta, M. Hybridizing Micro-Ti with Nano-B₄C Particulates to Improve the Microstructural and Mechanical Characteristics of Mg-Ti Composite *Journal of Magnesium and Alloys* 2 (1) 2014: pp. 13–19. <https://doi.org/10.1016/j.jma.2014.03.001>
7. Cafri, M., Dilman, H., Dariel, M.P., Frage, N. Boron Carbide/Magnesium Composites: Processing, Microstructure and Properties *Journal of European Ceramic Society* 32 (12) 2012: pp. 3477–3483. <https://doi.org/10.1016/j.jeurceramsoc.2012.04.007>

8. **Sankaranarayanan, S., Jayalakshmi, S., Gupta, M.** Effect of Individual and Combined Addition of Micro/Nano-sized Metallic Elements on the Microstructure and Mechanical Properties of Pure Mg *Materials and Design* 37 2012: pp. 274–284.
<https://doi.org/10.1016/j.matdes.2012.01.009>
9. **Perez, P., Garces, G., Adeva, P.** Mechanical Properties of a Mg–10 (vol. %) Ti Composite *Composite Science and Technology* 64 (1) 2004: pp. 145–151.
[https://doi.org/10.1016/S0266-3538\(03\)00215-X](https://doi.org/10.1016/S0266-3538(03)00215-X)
10. **Suryanarayana, C.** Mechanical Alloying and Milling *Progress in Materials Science* 46 (1–2) 2001: pp. 1–184.
[https://doi.org/10.1016/S0079-6425\(99\)00010-9](https://doi.org/10.1016/S0079-6425(99)00010-9)
11. **Sankar, C., Gangatharan, K., Christopher-Ezhil-Singh, S., Krishna Sharma, R., Mayandi, K.** Optimization on Tribological Behavior of Milled Nano B₄C Particles Reinforced with AZ91 Alloy Through Powder Metallurgy Method *Transactions of the Indian Institute of Metals* 72 (5) 2019: pp. 1255–1275.
<https://doi.org/10.1007/s12666-019-01618-y>
12. **Jaing, Q.C., Wank, H.Y., Ma, B.X., Wang, Y., Zhao, F.** Fabrication of B₄C Particulate Reinforced Magnesium Matrix Composite by Powder Metallurgy *Journal of Alloys and Compounds* 386 (1–2) 2015: pp. 177–181.
<https://doi.org/10.1016/j.jallcom.2004.06.015>
13. **Kaushik, N.C., Narasimha-Rao, R.** Two Body Abrasive Wear of Al-Mg-Si Hybrid Composites: Effect of Load and Sliding Distance *Materials Science (Medžiagotyra)* 22 (4) 2016: pp. 491–494.
<https://doi.org/10.5755/j01.ms.22.4.12688>
14. **Christopher-Ezhil-Singh, S., Selvakumar, N.** Effect of Milled B₄C Nanoparticles on Tribological Analysis, microstructure and mechanical Properties of Cu–4Cr Matrix Produced by Hot Extrusion *Archives of Civil and Mechanical Engineering* 17 (2) 2017: pp. 446–456.
<https://doi.org/10.1016/j.acme.2016.11.010>
15. **Narayanasamy, P., Selvakumar, N., Balasundar, P.** Effect of Hybridizing MoS₂ on the Tribological Behaviour of Mg–TiC Composites *Transaction of the Indian Institute of Metals* 68 (5) 2015: pp. 911–925.
<https://doi.org/10.1007/s12666-015-0530-z>



© Chinthamani et al. 2020 Open Access This article is distributed under the terms of the Creative Commons Attribution 4.0 International License (<http://creativecommons.org/licenses/by/4.0/>), which permits unrestricted use, distribution, and reproduction in any medium, provided you give appropriate credit to the original author(s) and the source, provide a link to the Creative Commons license, and indicate if changes were made.